Study of Ray Propagation Mechanisms in MultiStep Index Optical Fibers With Use in Computational Methods

Gotzon Aldabaldetreku, Gaizka Durana, Joseba Zubia, and Jon Arrue

Abstract—A comprehensive analysis of the various ray propagation mechanisms that take place between the different layers of highly multimode multistep index (MSI) fibers is presented. A suitable analytical expression that allows the evaluation of the power fraction transferred from a certain layer to another one from rays undergoing either refraction or frustrated total internal reflection is provided. This expression is valid for any MSI fiber of any number of layers with a radially decreasing refractive index profile. Frustrated total internal reflection is originated as a consequence of the discontinuous refractive index profile inherent in this type of fibers, and unlike in step-index and graded-index fibers, it can also affect bound rays. Such an expression will allow determination of the remaining ray power along the fiber in each possible propagation state created as a consequence of this phenomenon. The approximations made will be of great benefit for computational purposes since they will lead to a considerable simplification in the numerical prediction of ray propagation in these fibers.

Index Terms—Frustrated total internal reflection, geometric optics, multistep index (MSI) optical fibers, ray tracing.

I. INTRODUCTION

THE MOST significant characteristic of multistep index (MSI) fibers that differentiates them from their step-index (SI) or graded-index (GI) counterparts is their multilayered core: It comprises several layers of different refractive indexes that decrease as the radius increases in nearly all cases [1]. The possible application of these fibers, especially of the MSI polymer optical fibers (MSI-POFs), as a suitable transmission medium in short-haul communications links has recently been under consideration because they could serve as a complement to glass fibers or high-bandwidth GI polymer optical fibers (GI-POFs) [2]–[4].

A convenient way to classify rays in MSI fibers is to make use of the ray path equation, i.e., the equation that determines the range of values of the radial coordinate for which rays can propagate [5]. As a consequence, we have 1) bound rays (they are bound to the fiber core and do not leak into the cladding),

2) tunneling rays (they disappear in the core at the turning points and reappear in the cladding at a finite distance from the core-cladding interface), and 3) refracting rays (they cross the core-cladding interface) [1].

Nevertheless, because of the discontinuities in their refractive index profile, the ray path equation of MSI fibers is not a continuous function. This fact leads to three possible ray propagation mechanisms between the different layers within the core of MSI fibers. These mechanisms are based on the following phenomena: 1) total internal reflection, 2) refraction, and 3) frustrated total internal reflection [6]–[9].

It should be kept in mind that in the case of SI and GI fibers, the frustrated total internal reflection is only restricted to tunneling rays, whereas bound rays never experience such a propagation mechanism. In contrast, in MSI fibers, part of the ray power can be radiated to other layers even if the ray is bound to the fiber core, i.e., it does not leak into the cladding. Additionally, it is possible for a bound ray to refract to adjacent layers inside the core.

These two facts add great complexity to any computational method based on geometric optics that models ray propagation in MSI fibers since the number of rays that can be derived from a single ray is enormous and depends on the fiber length. The task of including all rays in a computational method is almost intractable; therefore, some approximations must be made.

In the case of refraction, the strategy to adopt is very simple. Considering that two rays appear from the incident ray, where one is reflected and the other one refracted [6], we will only choose the ray that conveys most of the energy. Thus, the only problem to solve in this case consists in determining the appropriate transmission coefficient. As will be observed later in the text, in all cases, the ray that is reflected back will convey a negligible amount of energy; consequently, it can be safely excluded from both the computational method and the final energy balance.

However, the case of rays undergoing frustrated total internal reflection deserves more careful consideration. As will be discussed later, it is very important in MSI fibers to assess accurately the effects of frustrated total internal reflection on every ray, especially on bound rays, since these effects could greatly modify the light propagation characteristics, depending on the fiber length.

In this paper, we intend to give a comprehensive analysis of such phenomena and to provide a suitable analytical expression for the evaluation of the power fraction radiated

between different layers by rays experiencing either refraction or frustrated total internal reflection. Such an expression will be derived by assuming that the refractive indexes of the layers decrease outward, which is the usual case in any kind of highly multimode fiber used as a transmission medium.

We will also provide the criteria for determining the propagation state in which a ray conveys most of its energy, which will lead to a considerable simplification in the analysis of ray propagation and will be advantageous for computational purposes.

II. DELIMITATION OF RAY PROPAGATION MECHANISMS IN TERMS OF RAY INVARIANTS

As stated in [1], the ray path equation $g(r)$ dictates that a ray can propagate within a certain layer i of constant refractive index n_i and outer radius ρ_i if

$$g(r)|_{r=\rho_i^-} = n_i^2 - \tilde{\beta}^2 - \frac{\tilde{l}^2 \rho_N^2}{\rho_i^2} > 0 \tag{1}$$

where the ray invariants $\tilde{\beta}$ and $\tilde{l}$ define the ray path

$$\tilde{\beta} = n_i \cos \theta_{z_i}$$

$$\tilde{l} = \frac{\rho_i}{\rho_N} n_i \sin \theta_{z_i} \cos \theta_{\phi_i}, \qquad i = 1, \ldots, N \tag{2}$$

where θ_{z_i} is the angle between the ray path and the longitudinal axis, and θ_{ϕ_i} is the angle between the ray path projection onto the fiber cross section and the azimuthal direction.

Since the refractive index n_i always remains constant within a certain layer (i.e., when $\rho_{i-1} < r \leqslant \rho_i$), the ray path equation increases monotonically with r until it reaches the outer radius ρ_i, in which case, it decreases again by a finite value (because $n_{i+1} < n_i$, since we have assumed typical MSI fibers, with radially decreasing refractive index profiles). Thus, a ray has a turning point $r_{tp} = \rho_i$ in a certain layer i when the following hold:

1) $g(r)|_{r=\rho_i^-} > 0 \Rightarrow n_i^2 - \tilde{\beta}^2 - \tilde{l}^2 \rho_N^2 / \rho_i^2 > 0 \Rightarrow n_i^2 > \tilde{\beta}^2 + \tilde{l}^2 \rho_N^2 / \rho_i^2$ (the ray does propagate in the ith layer);
2) $g(r)|_{r=\rho_i^+} < 0 \Rightarrow n_{i+1}^2 - \tilde{\beta}^2 - \tilde{l}^2 \rho_N^2 / \rho_i^2 < 0 \Rightarrow n_{i+1}^2 < \tilde{\beta}^2 + \tilde{l}^2 \rho_N^2 / \rho_i^2$ (the ray does not refract to the following layer, i.e., to the $(i+1)$th layer);

i.e., when

$$n_{i+1}^2 < \tilde{\beta}^2 + \frac{\tilde{l}^2 \rho_N^2}{\rho_i^2} < n_i^2 \Leftrightarrow r_{tp} = \rho_i. \tag{3}$$

However, this condition does not necessarily prevent the ray from propagating in the jth layer, with $j \geqslant i+1$ (note that j and i do not have to be necessarily consecutive layers). This is due to the fact that it is still possible in the jth layer that

$$g(r)|_{r=\rho_j^-} = n_j^2 - \tilde{\beta}^2 - \frac{\tilde{l}^2 \rho_N^2}{\rho_j^2} > 0.$$

Additionally, there is an inner caustic point for skew rays $(\tilde{l} \neq 0)$ in another layer h, with $h \leqslant i$, whose radius r_{ic} is given by [5]

$$g(r)|_{r_{ic}} = 0 \Rightarrow n_h^2 - \tilde{\beta}^2 - \frac{\tilde{l}^2 \rho_N^2}{r_{ic}^2} = 0$$

$$r_{ic}^2 = \frac{\tilde{l}^2 \rho_N^2}{n_h^2 - \tilde{\beta}^2} = \rho_h^2 \cos^2 \theta_{\phi_h}. \tag{4}$$

In contrast, there is no inner caustic for meridional rays $(\tilde{l} = 0)$ since (4) reduces to $r_{ic} = 0$.

In accordance with the previous considerations and taking into account that $n_{N+1} = n_{cl}$ (the refractive index of the cladding), the ray propagation between the layers of an MSI fiber is based on the following phenomena:

- *Total internal reflection*: Rays experiencing total internal reflection have a turning point $r_{tp} = \rho_i$ in a certain layer i and do not radiate further. They must satisfy one of the two following conditions:

$$\begin{cases} n_{i+1} \leqslant \tilde{\beta} \leqslant n_i; \\ 0 \leqslant \tilde{l} \leqslant \tilde{l}_{M,TR}(\tilde{\beta}); \end{cases} \qquad i = 1, \ldots, N \tag{5}$$

or

$$\begin{cases} \tilde{\beta}'_{min} \leqslant \tilde{\beta} < n_{i+1}; \\ \tilde{l}_{m,TR}(\tilde{\beta}) \leqslant \tilde{l} \leqslant \tilde{l}_{M,TR}(\tilde{\beta}); \end{cases} \qquad i = 1, \ldots, N-1 \tag{6}$$

where

$$\tilde{l}_{M,TR}^2(\tilde{\beta}) = \left(n_i^2 - \tilde{\beta}^2 \right) \frac{\rho_i^2}{\rho_N^2} \tag{7}$$

$$\tilde{l}_{m,TR}^2(\tilde{\beta}) = \left(n_{i+1}^2 - \tilde{\beta}^2 \right) \frac{\rho_{i+1}^2}{\rho_N^2} \tag{8}$$

$$\tilde{\beta}'_{min} = \max\{n_{cl}, \tilde{\beta}_{min}\} \tag{9}$$

and

$$\tilde{\beta}_{min}^2 = \begin{cases} \max\left\{0, \frac{\rho_{j+1}^2 n_{j+1}^2 - \rho_i^2 n_i^2}{\rho_{j+1}^2 - \rho_i^2}\right\}; & \begin{cases} i = 1, \ldots, N-1 \\ j = i, \ldots, N-1 \end{cases} \\ 0; & i = N. \end{cases} \tag{10}$$

These rays are always bound since $\tilde{\beta} \geqslant n_{cl}$.

- *Frustrated total internal reflection*: In this case, rays also have a turning point $r_{tp} = \rho_i$, even though they must satisfy simultaneously $\tilde{\beta}^2 < n_{i+1}^2$ and $n_{i+1}^2 < \tilde{\beta}^2 + \tilde{l}^2 \rho_N^2 / \rho_i^2$, or, to put it another way, one of the two following conditions must be fulfilled:

$$\begin{cases} \tilde{\beta}'_{min} \leqslant \tilde{\beta} < n_{i+1}; \\ \tilde{l}_{m,FR}(\tilde{\beta}) \leqslant \tilde{l} < \tilde{l}_{m,TR}(\tilde{\beta}); \end{cases} \qquad i = 1, \ldots, N-1 \tag{11}$$

or

$$\begin{cases} \tilde{\beta} < \tilde{\beta}'_{min}; \\ \tilde{l}_{m,FR}(\tilde{\beta}) \leqslant \tilde{l} \leqslant \tilde{l}_{M,TR}(\tilde{\beta}); \end{cases} \qquad i = 1, \ldots, N \tag{12}$$

where $\tilde{l}_{M,\mathrm{TR}}(\tilde{\beta})$, $\tilde{l}_{m,\mathrm{TR}}(\tilde{\beta})$, and $\tilde{\beta}'_{\min}$ are calculated using (7)–(9), respectively, and

$$\tilde{l}^2_{m,\mathrm{FR}}(\tilde{\beta}) = \begin{cases} \left(n^2_{i+1} - \tilde{\beta}^2\right)\dfrac{\rho^2_i}{\rho^2_N}; & i = 1,\ldots,N-1 \\ n^2_{\mathrm{cl}} - \tilde{\beta}^2; & i = N. \end{cases} \quad (13)$$

These rays can be bound, tunneling, or refracting. In any case, it is important to bear in mind that the conditions previously stated can only be satisfied by skew rays ($\tilde{l} \neq 0$).

For such rays, there is an electromagnetic radiation between $r_{\mathrm{tp}} = \rho_i$ and another radial coordinate $r > \rho_i$ satisfying $g(r) = 0$ since some energy leaks out at each turning point. We can incorporate this wave effect into our ray description by conveniently defining a power transmission coefficient and relating the amount of power radiation to the separation, or density, of reflection or the turning points along the fiber [5].

• *Refraction*: Rays refract from the ith to the $(i+1)$th layers, or vice versa, whenever they satisfy

$$\begin{cases} \tilde{\beta} < n_{i+1}; \\ 0 \leqslant \tilde{l} < \tilde{l}_{m,\mathrm{FR}}(\tilde{\beta}); \end{cases} \quad i = 1,\ldots,N \quad (14)$$

where $\tilde{l}_{m,\mathrm{FR}}(\tilde{\beta})$ is calculated using (13).

These rays can be bound, tunneling, or refracting.

As explained in the introduction, at the boundary between the ith and the $(i+1)$th layers, the incident ray splits into two rays: one reflected and the other one refracted [6]. We can make use of the same power transmission coefficient defined for rays undergoing frustrated total internal reflection, and we can extend its applicability to the calculation of the fraction of power conveyed by the reflected ray and the refracted one.

Obviously, if rays were meridional ($\tilde{l} = 0$), they would only experience either total internal reflection or refraction when propagating between the layers of an MSI fiber.

The following example illustrates the conditions that set the boundaries for the different phenomena discussed previously: Let us consider a parabolic-profile MSI fiber of ten layers with the typical characteristics of polymethylmethacrylate (PMMA)-based polymer optical fibers (POFs) [10]. We have chosen the value 1.492 as the refractive index of the innermost layer n_1 and 1.402 as the refractive index of the cladding n_{cl}. The radius of the outermost layer has been set to 490 μm. Notice that the election of such characteristics does not impose any constraint on the conclusions drawn from this analysis so that they can be easily extrapolated to any kind of highly multimode MSI fiber, provided that their refractive index profile decreases outward.

By maintaining the width of each layer constant ($\rho_i - \rho_{i-1} = \mathrm{constant}\ \forall i$), the corresponding refractive indexes have been adjusted so that the refractive index profile of the MSI fiber approximates the clad-parabolic one of a GI fiber, i.e.,

$$n_{\mathrm{MSI},i} = n_{\mathrm{GI}}(r)|_{r=\rho_{i-1}} \qquad \forall i \quad (\rho_0 = 0).$$
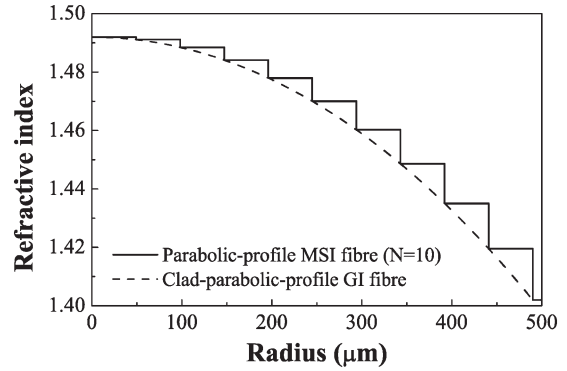

Fig. 1. Refractive index profile of a parabolic-profile MSI fiber of ten layers. The dashed line shows the profile of the clad-parabolic-profile GI fiber that we have used to adjust the refractive indexes of each layer.
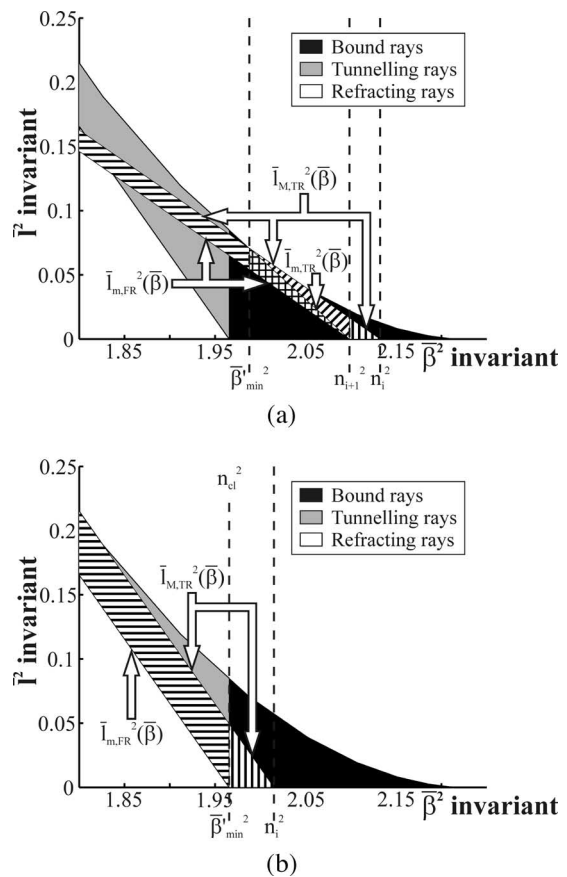

Fig. 2. Delineation of the regions corresponding to the different propagation mechanisms on the $\tilde{\beta}^2 - \tilde{l}^2$ plane, which is calculated for a parabolic-profile MSI fiber of ten layers. Depending on the values of $\tilde{\beta}$ and $\tilde{l}$, ray propagation from a certain layer i is based on total internal reflection [vertically and obliquely hatched regions, which satisfy (5) and (6), respectively], frustrated total internal reflection [crossed and horizontally hatched regions, which satisfy (11) and (12), respectively], or refraction [whole area below the limit line given by $\tilde{l}^2_{m,\mathrm{FR}}(\tilde{\beta})$ of (13)]. The black, gray, and white solid areas denote the regions for bound, tunneling, and refracting rays, respectively. (a) Ray propagating from the seventh layer. (b) Ray propagating from the tenth layer.

Fig. 1 shows the resultant parabolic refractive index profile for an MSI fiber of ten layers that is superimposed on the profile corresponding to a clad-parabolic-profile GI fiber.

The contour plots in Fig. 2 show the regions corresponding to the different ray propagation mechanisms on the $\tilde{\beta}^2 - \tilde{l}^2$
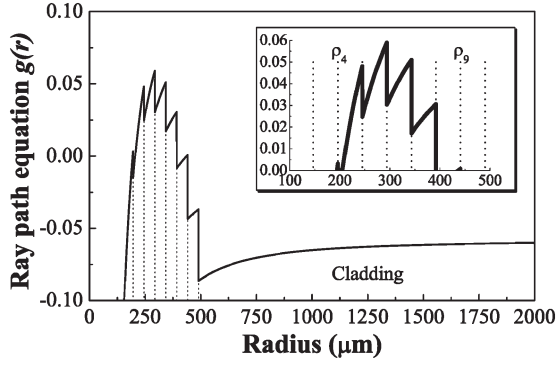
Fig. 3. Plot of the ray path equation $g(r)$ for a parabolic-profile MSI fiber of ten layers for $\tilde{\beta} = 1.4227$ and $\tilde{l} = 0.1675$. The inset shows a magnified view of $g(r)$. Layers are delimited by dotted vertical lines (see also Fig. 1).

TABLE I
RAY PATH CHARACTERISTICS FOR EACH PROPAGATION STATE OF A RAY PROPAGATING INSIDE A PARABOLIC-PROFILE MSI FIBER OF TEN LAYERS, WITH $\tilde{\beta} = 1.4227$ AND $\tilde{l} = 0.1675$

	r_{ic} (μm)	r_{tp} (μm)	z_p (μm)
1st propagation state	194.2 (Layer 4)	196 (Layer 4)	178.15
2nd propagation state	204.95 (Layer 5)	392 (Layer 8)	3230.53
(Ray refracts back and forth between the 5th and the 8th layers)			
3rd propagation state	436.52 (Layer 9)	441 (Layer 9)	948.99

plane for the preceding parabolic-profile MSI fiber of ten layers considered. Additionally, the black, gray, and white solid areas denote the regions for bound, tunneling, and refracting rays, respectively.

Let us now turn our attention to Fig. 2(a), which shows the boundaries of the regions for rays originating from the seventh layer. For values of $\tilde{\beta}$ and $\tilde{l}$ that belong to the vertically or obliquely hatched regions, rays experience total internal reflection at $r_{tp} = \rho_7$, so they do not radiate further (obviously, these rays are always bound to the fiber core). When the values of $\tilde{\beta}$ and $\tilde{l}$ lie within the crossed or horizontally hatched regions, rays undergo frustrated total internal reflection at $r_{tp} = \rho_7$. In this case, depending on the value of $\tilde{\beta}$, these rays can be bound, tunneling, or refracting. For $\tilde{\beta} \geqslant n_{cl}$, rays are bound to the fiber core, which means that although some energy leaks out to outer layers, this radiated energy will be retained by the fiber core in any of these layers (i.e., between the next one (eighth layer) and the outermost one) by means of total internal reflection. Instead, for $\tilde{\beta} < n_{cl}$, part of the ray power radiated to the outer layers is lost to the cladding afterward, either by means of a tunneling mechanism or by refraction. Finally, for values of $\tilde{l}$ such that $\tilde{l} < \tilde{l}_{m,FR}$, rays refract from the seventh layer to the following one (or vice versa). In this situation, depending on whether $\tilde{\beta} \geqslant n_{cl}$ is fulfilled or not, rays either are bound to the fiber core (i.e., they are retained by an outer layer by means of total internal reflection) or can radiate to the cladding (which is the case of tunneling or refracting rays).

On the other hand, Fig. 2(b) shows the particular case of rays originating from the outermost layer. Rays undergoing frustrated total internal reflection at $r_{tp} = \rho_{10}$ are always tunneling (horizontally hatched region), whereas rays refracted to the cladding are obviously refracting ($\tilde{l}_{m,FR}^2 = n_{cl}^2 - \tilde{\beta}^2$ corresponds to the limit where a tunneling ray becomes a refracting one). Finally, total internal reflection at $r_{tp} = \rho_{10}$ prevents bound rays from radiating to the outside of the fiber core (vertically hatched region). We would have obtained the same conclusions if we had considered an SI fiber with refractive index $n_{co} = n_{10}$ in the core.

If we now take the specific values of $\tilde{\beta} = 1.4227$ and $\tilde{l} = 0.1675$ and plot the corresponding ray path equation $g(r)$ in Fig. 3, it can be observed that it is possible for ray paths to exist within the fourth, fifth, sixth, seventh, eighth, or ninth layers.

Indeed, the inset reveals that $g(r)$ is positive even at the radial coordinates ρ_4 and ρ_9. However, since the ray path equation is a discontinuous function, there are values of r for which $g(r) < 0$ between ρ_4 and ρ_5 as well as between ρ_8 and ρ_9. This fact implies that the fields are no longer oscillatory but evanescent and, therefore, that rays are losing part of their power to outer layers by means of frustrated total internal reflection.

Suppose now that we launch a ray on the fourth layer at a certain radial position r between $r_{ic_4} = 194.2$ μm and $\rho_4 = 196$ μm with the values of $\tilde{\beta}$ and $\tilde{l}$ indicated previously. At each turning point $r_{tp} = \rho_4$, evanescent fields transfer part of the ray power to the next radiation caustic, which coincides with the inner caustic of the ray in the fifth layer ($r_{ic_5} = 204.95$ μm). A ray propagating in the fifth layer can also reach the eighth layer by means of successive refractions (in which case, $r_{tp} = \rho_8 = 392$ μm). Here, the ray experiences a frustrated total internal reflection again, so part of its power will be radiated to the ninth layer (at $r_{ic_9} = 436.52$ μm). Since rays reaching the ninth layer satisfy the total internal reflection condition stated in (5), there will be no further leakage beyond $r_{tp} = \rho_9 = 441$ μm, which means that the ray is truly bound to the fiber core since $\tilde{\beta} = 1.4227 > n_{cl} = 1.402$.

All in all, we can identify three possible propagation states: The first one is within the fourth layer; the second one is between the fifth and the eighth layers; and the third one is in the ninth layer. It is clear that the possible excitation of the ray in one of these three allowed propagation states strongly depends on the launching conditions, with the probability of exciting the ray in the second propagation state being higher than in the rest of the cases, as can be deduced from the inset in Fig. 3.

For convenience, all these results have been summarized in Table I, which also shows the ray half-period corresponding to each propagation state. The ray half-period, which is denoted by z_p, is the axial distance between successive turning points [1].

As will be discussed in Section III, rays experiencing refraction convey practically all of their energy to the adjacent layer even if we considered distances in the order of the corresponding ray half-period. In contrast, we will see that rays undergoing frustrated total internal reflection have very low power transfer rates in general. As a result, in the case of the previous example, it is expected that for short lengths of fiber, a ray propagating in the fourth layer will retain most of its initial power, whereas this initial power will be completely transferred to the ninth layer for sufficiently long distances. In between,
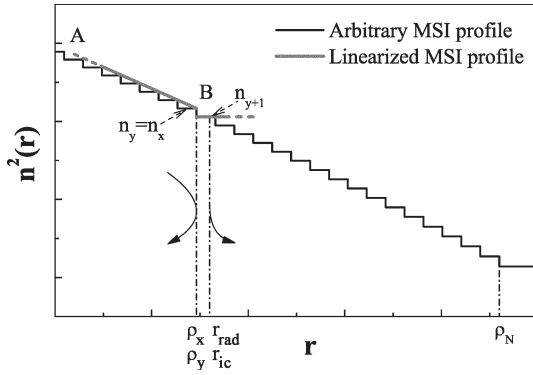
Fig. 4. Linearized profile used in the analysis corresponding to $\overline{AB}$ (gray line). At ρ_x, the ray is partially reflected, and the position $r_{\rm rad}$ stands for the point where the transmitted ray reappears. It also corresponds to the inner caustic $r_{\rm ic}$ of the ray propagating in the $(y+1)$th layer. In this example, the ray has its turning point in the layer preceding the one to which it radiates; thus, $\rho_y = \rho_x$.

the ray will gradually undergo a leakage from the fourth to the fifth layers, giving rise to a new ray that also leaks to the ninth layer whenever it reaches the eighth one after successive refractions, and so on. Both issues will be discussed in detail in Section IV.

III. POWER TRANSMISSION COEFFICIENT FOR RAYS UNDERGOING FRUSTRATED TOTAL INTERNAL REFLECTION OR REFRACTION

We have already discussed the usefulness of defining a power transmission coefficient T and providing an analytical expression for its calculation in a similar way to a study carried out for tunneling and refracting rays [5]. Such an expression would allow us to determine the power attenuation γ experienced by a ray at each turning point and to assess the remaining ray power $P(z)$ along the fiber in each possible propagation state [11], [12], i.e.,

$$\gamma = T/z_p$$
$$P(z) = P(0)\exp(-\gamma z).$$

We can make use of the transmission coefficient for tunneling and refracting rays in MSI fibers given in [13, eq. (33)], provided that we conveniently adapt it with some minor modifications. Such an expression is based on the method of uniform approximation and has been successfully applied to tunneling and refracting rays in SI and GI fibers as well [14].

Once again, the derivation of such a power transmission coefficient relies on the linearization of the square of the core refractive index of the MSI fiber [11], [15], but this time, this task must be done at the top of the jump at $r = \rho_y$, with y being the layer preceding the one to which the ray radiates. We are assuming that in the preceding propagation state, the ray has its turning point in a certain layer $x \leqslant y$ at $r_{\rm tp} = \rho_x$. This is shown in Fig. 4. Note that layers x and $y+1$ (the layer to which the ray radiates) do not have to be consecutive, or to put it another way, it is possible for the ray to "tunnel" through a certain number of layers.

From the linearization, we obtain

$$n^2(r) = \begin{cases} \delta(r-\rho_y) + n_y^2; & r \lesssim \rho_y \\ n_{y+1}^2; & r \gtrsim \rho_y \end{cases}, \qquad (n_{N+1} = n_{\rm cl}) \tag{15}$$

where n_y is the refractive index, and ρ_y is the outer radius of the yth layer [i.e., the ray radiates to the $(y+1)$th layer]. The value of δ is the slope of the core profile at $r = \rho_y^-$

$$\delta = \left.\frac{dn^2(r)}{dr}\right|_{r=\rho_y^-} = \frac{n_y^2 - n_{y-1}^2}{\rho_y - \rho_{y-1}} \tag{16}$$

and it turns out that $\delta < 0$ since we are assuming that the refractive index profile decreases with r.

Obviously, if $y = N$, the ray will leak to the cladding (i.e., it will reappear at a finite distance from the core-cladding interface if it undergoes frustrated total internal reflection, or it will simply refract to the cladding if it experiences refraction). In this case $(y = N)$, the power transmission coefficient reduces to that corresponding to tunneling and refracting rays, as discussed in [13]. It must be pointed out that we have assumed, for the sake of simplicity, that the cladding extends to infinity.

We summarize the new analytical expressions that replace some of the original expressions used in [13] to calculate the power transmission coefficient derived from the uniform method. Such modifications make it possible to use T in [13, eq. (33)] to calculate the power transmission coefficient for rays undergoing either frustrated total internal reflection or refraction in MSI fibers, as follows.

- First, the k_{r_1}, k_{r_2}, k'_{r_1}, and k'_{r_2} given in [13, eqs. (24), (25), (36) and (37)], respectively, are replaced by (17) and (18), shown at the bottom of the next page. In the preceding equations, δ is now the slope of the core profile evaluated at $r = \rho_y^-$ [which is given by (16)].
- Second, the ξ_1 given in [13, eq. (34)] is evaluated by performing a numerical integration of $k_{r_1}(r)$ (in [13, eq. (24)]), but this time, we must use the linearized profile given by (15). One of the limits of the original integral ρ_N is substituted with ρ_y. The other limit, i.e., the turning point $r_{\rm tp}$ corresponding to the linearized profile, is calculated by using [13, eq. (26)], even though the original parameters a and b are now updated according to

$$a = \delta$$
$$b = -\delta\rho_y + n_y^2 - \tilde{\beta}^2.$$

[Again, δ is the slope of the core profile given by (16). Note also that the parameter c in [13] is still equal to $-\tilde{l}^2\rho_N^2$].
- Finally, the ξ_2 given in [13, eq. (35)] is replaced by (19), shown at the bottom of the next page.

The maximum allowed value of $\tilde{l}$ for the linearized profile in (15) is given by

$$\tilde{l}_{max}^2(\tilde{\beta}) = \frac{4}{27\delta^2\rho_N^2}\left[-\delta\rho_y - \left(\tilde{\beta}^2 - n_y^2\right)\right]^3 \tag{20}$$

which, in some cases, could be slightly lower than that corresponding to the original discontinuous profile (see [13, eq. (7)]). Again, we can make use of the expression derived from the Wentzel–Kramer–Brillouin (WKB) approximation, which is given in [13, eq. (43)]. In this case, we only need to make the following changes.

- Replace the upper limit N of the product in [13, eq. (43)] with y.
- Replace the upper limit N of the sum in [13, eq. (46)] with y.
- Replace ζ_2 given in [13, eq. (47)] by

$$\zeta_2 = -2k\rho_N \left\{ \tilde{l} \ln \left[\frac{\frac{\tilde{l}\rho_N}{\rho_y} + \left(\tilde{\beta}^2 + \frac{\tilde{l}^2 \rho_N^2}{\rho_y^2} - n_{y+1}^2 \right)^{1/2}}{\left(n_{y+1}^2 - \tilde{\beta}^2 \right)^{1/2}} \right] - \left[\tilde{l}^2 + \frac{\rho_y^2}{\rho_N^2} \left(\tilde{\beta}^2 - n_{y+1}^2 \right) \right]^{1/2} \right\}. \quad (21)$$

Following a similar reasoning as that stated in [13], we can conclude that the results for T based on the WKB solutions of

the scalar wave equation introduce a negligible error into the calculation of the power attenuation along the fiber.

Finally, we can also extend the definition of the power transmission coefficient based on the WKB solutions for rays undergoing refraction between successive layers, if we replace [13, eq. (48)] by

$$T_{\text{refr}} = 4 \left[\left(n_y^2 - \tilde{\beta}^2 - \frac{\tilde{l}^2 \rho_N^2}{\rho_y^2} \right) \left(n_{y+1}^2 - \tilde{\beta}^2 - \frac{\tilde{l}^2 \rho_N^2}{\rho_y^2} \right) \right]^{1/2}$$

$$\div \left\{ \left(n_y^2 - \tilde{\beta}^2 - \frac{\tilde{l}^2 \rho_N^2}{\rho_y^2} \right) + \left(n_{y+1}^2 - \tilde{\beta}^2 - \frac{\tilde{l}^2 \rho_N^2}{\rho_y^2} \right) \right.$$

$$+ 2 \left[\left(n_y^2 - \tilde{\beta}^2 - \frac{\tilde{l}^2 \rho_N^2}{\rho_y^2} \right) \right.$$

$$\left. \left. \times \left(n_{y+1}^2 - \tilde{\beta}^2 - \frac{\tilde{l}^2 \rho_N^2}{\rho_y^2} \right) \right]^{1/2} \right\} \quad (22)$$

which is the classical Fresnel transmission coefficient adapted for our case [16], [17].

$$\begin{cases} \text{if } n_y^2 > \tilde{\beta}^2 + \frac{\tilde{l}^2 \rho_N^2}{\rho_y^2} \text{ then} \begin{cases} k_{r_1} = k \left(n_y^2 - \tilde{\beta}^2 - \frac{\tilde{l}^2 \rho_N^2}{\rho_y^2} \right)^{1/2}, \\ k'_{r_1} = k \frac{\frac{\tilde{l}^2 \rho_N^2}{\rho_y^3} + \frac{\delta}{2}}{\left(n_y^2 - \tilde{\beta}^2 - \frac{\tilde{l}^2 \rho_N^2}{\rho_y^2} \right)^{1/2}}, \end{cases} \Rightarrow k_{r_1}^2 > 0 \\ \text{if } n_y^2 < \tilde{\beta}^2 + \frac{\tilde{l}^2 \rho_N^2}{\rho_y^2} \text{ then} \begin{cases} k_{r_1} = \imath k \left(\tilde{\beta}^2 + \frac{\tilde{l}^2 \rho_N^2}{\rho_y^2} - n_y^2 \right)^{1/2}, \\ k'_{r_1} = \imath k \frac{-\frac{\tilde{l}^2 \rho_N^2}{\rho_y^3} - \frac{\delta}{2}}{\left(\tilde{\beta}^2 + \frac{\tilde{l}^2 \rho_N^2}{\rho_y^2} - n_y^2 \right)^{1/2}}, \end{cases} \Rightarrow k_{r_1}^2 < 0 \end{cases} \quad (17)$$

$$\begin{cases} \text{if } n_{y+1}^2 > \tilde{\beta}^2 + \frac{\tilde{l}^2 \rho_N^2}{\rho_y^2} \text{ then} \begin{cases} k_{r_2} = k \left(n_{y+1}^2 - \tilde{\beta}^2 - \frac{\tilde{l}^2 \rho_N^2}{\rho_y^2} \right)^{1/2}, \\ k'_{r_2} = k \frac{\frac{\tilde{l}^2 \rho_N^2}{\rho_y^3}}{\left(n_{y+1}^2 - \tilde{\beta}^2 - \frac{\tilde{l}^2 \rho_N^2}{\rho_y^2} \right)^{1/2}}, \end{cases} \Rightarrow k_{r_2}^2 > 0 \\ \text{if } n_{y+1}^2 < \tilde{\beta}^2 + \frac{\tilde{l}^2 \rho_N^2}{\rho_y^2} \text{ then} \begin{cases} k_{r_2} = \imath k \left(\tilde{\beta}^2 + \frac{\tilde{l}^2 \rho_N^2}{\rho_y^2} - n_{y+1}^2 \right)^{1/2}, \\ k'_{r_2} = \imath k \frac{-\frac{\tilde{l}^2 \rho_N^2}{\rho_y^3}}{\left(\tilde{\beta}^2 + \frac{\tilde{l}^2 \rho_N^2}{\rho_y^2} - n_{y+1}^2 \right)^{1/2}}, \end{cases} \Rightarrow k_{r_2}^2 < 0 \end{cases} \quad (18)$$

$$\begin{cases} \text{if } k_{r_2}^2 > 0 \text{ then } \xi_2 = - \left[\frac{3}{2} k \rho_N \left\{ \left[\frac{\rho_y^2}{\rho_N^2} \left(n_{y+1}^2 - \tilde{\beta}^2 \right) - \tilde{l}^2 \right]^{1/2} - \tilde{l} \arccos \left[\frac{\frac{\tilde{l}\rho_N}{\rho_y}}{\left(n_{y+1}^2 - \tilde{\beta}^2 \right)^{1/2}} \right] \right\} \right]^{2/3} \\ \text{if } k_{r_2}^2 < 0 \text{ then } \xi_2 = + \left[\frac{3}{2} k \rho_N \left\{ \tilde{l} \ln \left[\frac{\frac{\tilde{l}\rho_N}{\rho_y} + \left(\tilde{\beta}^2 + \frac{\tilde{l}^2 \rho_N^2}{\rho_y^2} - n_{y+1}^2 \right)^{1/2}}{\left(n_{y+1}^2 - \tilde{\beta}^2 \right)^{1/2}} \right] - \left[\tilde{l}^2 + \frac{\rho_y^2}{\rho_N^2} \left(\tilde{\beta}^2 - n_{y+1}^2 \right) \right]^{1/2} \right\} \right]^{2/3} \end{cases} \quad (19)$$

TABLE II
POWER TRANSMISSION COEFFICIENT T CALCULATED FOR A RAY
UNDERGOING REFRACTION WHEN IT PROPAGATES INSIDE A
PARABOLIC-PROFILE MSI FIBER OF TEN LAYERS, WITH
$\tilde{\beta} = 1.4227$ AND $\tilde{l} = 0.1675$. WE USE THE NOTATION
"$i \to (i + 1)$", WITH i BEING AN INTEGER, TO
INDICATE THAT EACH INDIVIDUAL RESULT
CORRESPONDS TO A RAY REFRACTING
FROM THE iTH LAYER TO THE
FOLLOWING $(i + 1)$TH ONE

	T (uniform method)	T (WKB approximation)
$5 \to 6$	0.972 70	0.972 69
$6 \to 7$	0.972 88	0.972 88
$7 \to 8$	0.929 34	0.929 33

IV. DISCUSSION

Let us consider again a bound ray with the invariant values $\tilde{\beta} = 1.4227$ and $\tilde{l} = 0.1675$ but this time launched on the fifth layer of the parabolic-profile MSI fiber of ten layers shown in Fig. 1. More specifically, this ray is launched at a certain radial position r between $r_{ic_5} = 204.95\ \mu m$ and $\rho_5 = 245\ \mu m$.

In Section II, we have already seen that according to the ray path equation $g(r)$, such a ray refracts back and forth between this layer and the eighth one (on each refraction, the incident ray splits into two rays: one reflected and another one refracted), and it radiates part of its energy to the ninth layer whenever it reaches $r_{tp} = \rho_8$ by means of frustrated total internal reflection. In this particular case, we are interested in assessing how high the value of the power transmission coefficient T is for each refraction in order to seek appropriate approximations that will facilitate the implementation of computational methods to predict light propagation in MSI fibers. For this purpose, in Table II, we have calculated the results obtained for the power transmission coefficient T for each refraction (the refracted ray conveys the fraction T of the incident ray power, whereas the reflected ray retains the fraction of power $1 - T$). To calculate T, we have used both the expressions derived from the uniform method and the WKB approximation.

In all cases, it is found that the power transmission coefficient is so high that the remaining power conveyed by the ray reflected back is practically negligible in comparison with the refracted power. For instance, if we consider the refraction from the fifth to the sixth layers, the percentage of power reflected back will only be $100 - 97.27 = 2.73\%$. If we followed the trajectory of the reflected ray inside the fifth layer, instead of simply rejecting it, until the following refraction occurs (which happens when the ray has covered the very short axial distance of $z = 953.82\ \mu m$), we would obtain that the fraction of power remaining in this layer would be even smaller. As a consequence, it is expected that excluding the reflected ray will introduce a negligible amount of error in the calculation of the final ray power distribution. Such an approximation leads to a considerable simplification in the numerical prediction of ray propagation, which is also considerably advantageous from a computational point of view.

Let us now turn our attention again to the case of frustrated total internal reflection, considering the bound ray used at the end of Section II (with $\tilde{\beta} = 1.4227$ and $\tilde{l} = 0.1675$) when it is launched on the fourth layer of the parabolic-profile MSI fiber

TABLE III
POWER TRANSMISSION COEFFICIENT T AND POWER ATTENUATION γ
CALCULATED FOR A RAY UNDERGOING FRUSTRATED TOTAL INTERNAL
REFLECTION WHEN IT PROPAGATES INSIDE A PARABOLIC-PROFILE MSI
FIBER OF TEN LAYERS, WITH $\tilde{\beta} = 1.4227$ AND $\tilde{l} = 0.1675$. WE USE
THE NOTATION "$i \to j$", WITH i AND j BEING INTEGERS, TO INDICATE
THAT THE OBTAINED RESULTS ARE A CONSEQUENCE OF THE RAY
RADIATION POWER TAKING PLACE FROM THE iTH LAYER TO THE
jTH ONE. $P(z)/P(0)$ INDICATES THE REMAINING POWER AT A
DISTANCE z FOR A RAY PROPAGATING IN A PROPAGATION
STATE FOR WHICH $r_{tp} = \rho_i$ (I.E., THE RAY HAS ITS
TURNING POINT IN THE iTH LAYER)

Results obtained using the uniform method				
	T	γ	$P(z)/P(0)$	
			$z = 1$ m	$z = 100$ m
$4 \to 5$	1.669×10^{-6}	9.369×10^{-3}	9.907×10^{-1}	3.918×10^{-1}
$8 \to 9$	1.024×10^{-22}	3.171×10^{-20}	1.0	1.0

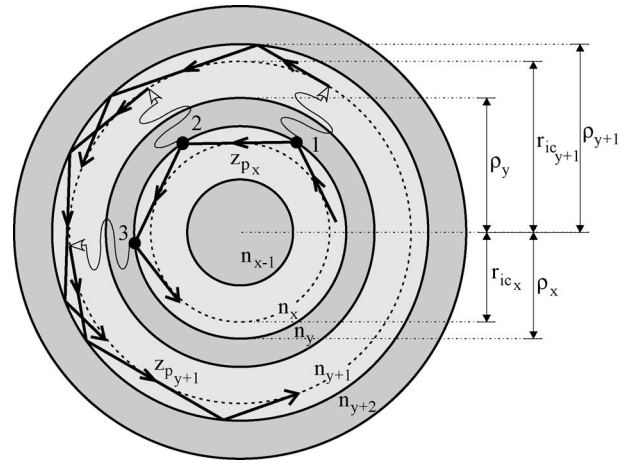| Results obtained using the WKB approximation				
	T	γ	$P(z)/P(0)$	
			$z = 1$ m	$z = 100$ m
$4 \to 5$	1.375×10^{-6}	7.719×10^{-3}	9.923×10^{-1}	4.621×10^{-1}
$8 \to 9$	1.029×10^{-22}	3.184×10^{-20}	1.0	1.0

Fig. 5. Projection of the ray paths onto the core cross section of an MSI fiber. A ray propagating in the xth layer undergoes frustrated total internal reflection each time it reaches the turning point ρ_x at points 1, 2, and 3. From each turning point, an evanescent field transfers part of its power to the following propagation state in the $(y + 1)$th layer, giving rise to a new ray. z_{p_x} is the ray half-period corresponding to the ray propagating in the initial propagation state, whereas $z_{p_{y+1}}$ corresponds to the ray half-period of each of the rays emerging in the following propagation state.

of ten layers. Table III reproduces the results obtained for the power transmission coefficient T and the power attenuation γ when the ray undergoes frustrated total internal reflection at $r_{tp} = \rho_4$ from the fourth to the fifth layers and at $r_{tp} = \rho_8$ from the eighth to the ninth layers (refer back to Table I for further details). Table III also shows the remaining ray power $P(z)$ in each of the first two propagation states, which is related to the initial power $P(0)$ and calculated for two different fiber lengths: $z = 1$ and 100 m. The results have been calculated using both the expressions derived from the uniform method and the WKB approximation.

As anticipated at the end of Section II, each time that a ray undergoing frustrated total internal reflection reaches the turning point, two rays are created. This is best illustrated in Fig. 5.

It shows a ray that propagates in a certain propagation state and has its inner caustic at r_{ic_x}. In this example, points 1–3 are three consecutive points where the ray reaches the turning point at ρ_x. From each of these points, an evanescent field that carries part of its power to the $(y + 1)$th layer emerges, giving rise to a new ray that propagates in the following propagation state. Now, this new ray has its inner caustic at $r_{ic_{y+1}}$, whereas its turning point is at ρ_{y+1}.

We should notice that if there are more than two possible propagation states, the analysis could become intractable since at successive turning points, each ray generates a lot of new radiated rays, with their number depending on the fiber length. Nevertheless, only a few of them must be considered, i.e., those that convey most of the energy. Therefore, we have adopted the following criterion to select rays: If a ray propagating in a certain propagation state has a ratio $P(z)/P(0)$ lower than 0.5 at a certain distance z (meaning that more than 50% of its power has been radiated to outer layers), we choose the following possible propagation state to continue. Otherwise, we restrict our analysis to the current propagation state and ignore the rest of them. Such an approximation simplifies considerably the analysis of ray propagation in MSI fibers, and it is also of great benefit for computational purposes.

If we refer back to the results obtained using the uniform method in Table III, it can be observed that for a fiber length of $z = 1$ m, a ray propagating in the first propagation state (in the fourth layer) retains most of its power (specifically, 99.07%), whereas a ray excited in the second propagation state would hardly lose energy. However, if we now take a fiber length of $z = 100$ m, then a ray that initially started propagating in the first propagation state would lose $100 - 39.18 = 60.82\%$ of its power, whereas a ray propagating in the second propagation state would still retain most of its initial power. In this case, we would choose the second propagation state as the appropriate one. Only for a fiber length sufficiently large would all the ray power be practically conveyed to the third propagation state, irrespective of the initial propagation state.

Additionally, it would be particularly interesting to calculate the power transmission coefficient T when a bound ray experiencing frustrated total internal reflection approximates the limit where it would start to refract to the following layer, with a view of confirming whether it is a reasonable value or not. While maintaining the value of $\tilde{\beta}$ fixed and using the same ray parameters as in the previous examples (i.e., $\tilde{\beta} = 1.4227$, and the ray is launched on the fourth layer of the parabolic-profile MSI fiber of ten layers), this limit is achieved when $\tilde{l} \to \tilde{l}_{m,\text{FR}}(1.4227) = 1.6019 \times 10^{-1}$. Under such circumstances, we would obtain $T = 0.6451$ and $\gamma = 1530.4 \text{ m}^{-1}$ for the first propagation state (note that the ray half-period corresponding to this propagation state is now $z_p = 421.53$ μm). It turns out that the distance z at which more than 50% of the initial power is radiated to the fifth layer (in which case we will select the second propagation state in the ray propagation analysis) is only 452.92 μm, i.e., in the order of the ray-half period corresponding to the first propagation state. This means that as expected, the initial power launched on the fourth layer is extremely rapidly transferred to the fifth one. Consequently, as the value of $\tilde{\beta}$ or $\tilde{l}$ decreases and T increases

(when the frustrated total internal reflection between the fourth and fifth layers becomes refraction), this power transfer will be almost complete. This fact is also consistent with the line of reasoning followed in the approximation made for rays undergoing refraction, which consisted in neglecting the amount of energy retained by a ray reflected at the interface between two consecutive layers.

Another conclusion can also be drawn from both Tables II and III, as it is noticeable that the results obtained using the expressions based on the WKB solutions of the scalar wave equation are in good agreement with those derived from the uniform method. Indeed, the WKB representations are highly accurate for practically all rays experiencing either frustrated total internal reflection or refraction, provided that they are not very close to the limit $\tilde{l}_{m,\text{FR}}^2(\tilde{\beta})$ [13].

V. CONCLUSION

In this paper, we have identified and delimited the three possible ray propagation mechanisms that take place between the different layers within the core of MSI fibers with radially decreasing refractive index profiles. We have observed that as a result of their discontinuous refractive index profile, it is possible, even for bound rays, for part of the ray power to be radiated to other layers by means of either refraction or frustrated total internal reflection. This fact leads to different possible propagation states, which are subjected to the launching conditions, to the power transfer rate of the ray and to the fiber length. We have derived the appropriate expressions for the power transmission coefficient that allow us to calculate the remaining ray power along the fiber in each propagation state and, in this way, aid us in selecting the propagation state in which a ray conveys most of its energy. These approximations lead to a considerable simplification in the numerical prediction of ray propagation in MSI fibers, making it possible to implement simple and accurate computational methods based on geometric optics.

REFERENCES

[1] J. Zubia, G. Aldabaldetreku, G. Durana, J. Arrue, H. Poisel, and C. A. Bunge, "Geometric optics analysis of multi-step index optical fibers," *Fiber Integr. Opt.*, vol. 23, no. 2/3, pp. 121–156, Mar./Jun. 2004.

[2] K. Irie, Y. Uozu, and T. Yoshimura, "Structure design and analysis of broadband POF," in *Proc. 10th Int. Conf. POF and Applications*, Amsterdam, The Netherlands, Sep. 2001, pp. 73–79.

[3] T. Ishigure, M. Sato, A. Kondo, and Y. Koike, "High-bandwidth graded-index polymer optical fiber with high temperature stability," *J. Lightw. Technol.*, vol. 20, no. 8, pp. 1443–1448, Aug. 2002.

[4] T. Ishigure, K. Makino, S. Tanaka, and Y. Koike, "High-bandwidth graded-index plastic optical fiber enabling power penalty-free gigabit data transmission," *J. Lightw. Technol.*, vol. 21, no. 11, pp. 2923–2930, Nov. 2003.

[5] A. W. Snyder and J. D. Love, *Optical Waveguide Theory*. London, U.K.: Chapman & Hall, 1983.

[6] M. Born and E. Wolf, *Principles of Optics*, 6 ed. New York: Pergamon, 1990.

[7] S. Zhu, A.W. Yu, D. Hawley, and R. Roy, "Frustrated total internal reflection: A demonstration and review," *Amer. J. Phys.*, vol. 54, no. 7, pp. 601–606, Jul. 1986.

[8] F. P. Zanella, D. V. Magalhães, M. M. Oliveira, R. F. Bianchi, L. Misoguti, and C. R. Mendona, "Frustrated total internal reflection: A simple application and demonstration," *Amer. J. Phys.*, vol. 71, no. 5, pp. 494–496, May 2003.

[9] A. A. Stahlhofen, "Comment on frustrated total internal reflection: A simple application and demonstration," *Amer. J. Phys.*, vol. 72, no. 3, p. 412, Mar. 2004.

[10] J. Zubia and J. Arrue, "Plastic optical fibers: An introduction to their technological processes and applications," *Opt. Fiber Technol.*, vol. 7, no. 2, pp. 101–140, Apr. 2001.

[11] J. D. Love and C. Winkler, "Attenuation and tunneling coefficients for leaky rays in multilayered optical waveguides," *J. Opt. Soc. Amer.*, vol. 67, no. 12, pp. 1627–1632, Dec. 1977.

[12] A. W. Snyder and D. J. Mitchell, "Generalized Fresnel's laws for determining radiation loss from optical waveguides and curved dielectric structures," *Optik*, vol. 40, no. 4, pp. 438–459, 1974.

[13] G. Aldabaldetreku, J. Zubia, G. Durana, and J. Arrue, "Power transmission coefficients for multi-step index optical fibres," *Opt. Express*, vol. 14, no. 4, pp. 1413–1429, Feb. 2006. [Online]. Available: http://www.opticsexpress.org/abstract.cfm?URI=oe-14-4-1413

[14] J. D. Love and C. Winkler, "A universal tunnelling coefficient for step- and graded-index multimode fibres," *Opt. Quantum Electron.*, vol. 10, no. 4, pp. 341–351, 1978.

[15] ——, "Refracting leaky rays in graded-index fibers," *Appl. Opt.*, vol. 17, no. 14, pp. 2205–2208, Jul. 1978.

[16] A. W. Snyder and J. D. Love, "Reflection at a curved dielectric interface—Electromagnetic tunneling," *IEEE Trans. Microw. Theory Tech.*, vol. MTT-23, no. 1, pp. 134–141, Jan. 1975.

[17] J. D. Love and A. W. Snyder, "Fresnel's and Snell's laws for the multimode optical waveguide of circular cross section," *J. Opt. Soc. Amer.*, vol. 65, no. 11, pp. 1241–1247, Nov. 1975.

Gotzon Aldabaldetreku received the M.Sc. degree in telecommunications engineering from the University of the Basque Country, Bilbao, Spain, in 2000. He is currently working toward the Ph.D. degree in theoretical analysis of multi-step index fibers at the University of the Basque Country.

For nearly six years, he has been doing research on optical fibers at the Department of Electronics and Telecommunications, School of Engineering of Bilbao, University of the Basque Country, where he became an Assistant Lecturer in 2002.

Gaizka Durana received the M.Sc. degree in solid-state physics from the University of the Basque Country, Bilbao, Spain, in 1999. He is currently working toward the Ph.D. degree in the study of light polarization properties in polymer optical fibers at the University of the Basque Country.

He is currently a Lecturer and a Researcher with the Department of Electronics and Telecommunications, School of Engineering of Bilbao, University of the Basque Country.

Joseba Zubia received the M.Sc. degree in solid-state physics and the Ph.D. degree in physics from the University of the Basque Country, Bilbao, Spain, in 1988 and 1993, respectively. His Ph.D. work focused on the optical properties of ferroelectric liquid crystals.

He is currently a Full Professor with the Department of Electronics and Telecommunications, School of Engineering of Bilbao, University of the Basque Country. He has more than 11 years of experience doing basic research in the field of polymer optical fibers and is currently involved in research projects in collaboration with universities and companies from Spain and other countries in the field of polymer optical fibers, fiber-optic sensors, and liquid crystals.

Prof. Zubia was a recipient of a special award for Best Thesis in 1995.

Jon Arrue received the M.Sc. degree in electronic physics, completed a 12-month postgraduate course in electronics and a 12-month postgraduate course in telecommunications, and received the Ph.D. degree in optical fibers from the University of the Basque Country, Bilbao, Spain, in 1990, 1991, 1992, and 2001, respectively.

He is currently a Professor with the Department of Electronics and Telecommunications, School of Engineering of Bilbao, University of the Basque Country, and is also involved in international research projects with other universities and companies.

Dr. Arrue was a recipient of a special award for his thesis and a European acknowledgement of the Ph.D. degree.